Conductivity Mechanism in Polymerized Imidazolium-Based Protic Ionic Liquid [HSO3-BVIm][OTf]: Dielectric Relaxation Studies

ARTICLE *in* MACROMOLECULES · JUNE 2014

Impact Factor: 5.8 · DOI: 10.1021/ma5003479

6 AUTHORS, INCLUDING:

Mariana Díaz
Universidad de Cantabria
6 PUBLICATIONS **48** CITATIONS
SEE PROFILE

Inmaculada Ortiz
Universidad de Cantabria
289 PUBLICATIONS **5,438** CITATIONS
SEE PROFILE

Macromolecules

Article

pubs.acs.org/Macromolecules

Conductivity Mechanism in Polymerized Imidazolium-Based Protic Ionic Liquid [HSO_3−BVIm][OTf]: Dielectric Relaxation Studies

Z. Wojnarowska,*[,†,‡] J. Knapik,[†,‡] M. Díaz,[§] A. Ortiz,[§] I. Ortiz,[§] and M. Paluch[†,‡]

[†]Institute of Physics, University of Silesia, Uniwersytecka 4, 40-007 Katowice, Poland

[‡]SMCEBI 75 Pułku Piechoty 1A, 41-500 Chorzow, Poland

[§]Department of Chemical and Biomolecular Engineering, University of Cantabria, Santander, Spain

ABSTRACT: In this paper, we investigate the molecular dynamics and ions transport properties of polymerized imidazolium-based protic ionic liquid [HSO_3−BVIm][OTf]—a new material with potential applications in energy storage and electrochemical devices. The results of dielectric measurements, analyzed in modulus $M^*(f)$ and conductivity $\sigma^*(f)$ formalisms, combined with temperature-modulated differential scanning calorimetry experiments, have revealed a fundamental difference between the conducting properties of the examined polymer membrane and its low-molecular weight counterpart. Our findings indicated a strong decoupling between conductivity relaxation times τ_σ (related to the ions migration through the polymer matrix) and segmental dynamics when the ionic transport is controlled by fast proton hopping through the dense hydrogen-bond network. Finally, we also discuss, for the first time, the effect of water content on the glass transition temperature value, relation between the charge and mass diffusion, reflected in the decoupling phenomenon, and the conductivity mechanism of examined poly[HSO_3−BVIm][OTf].

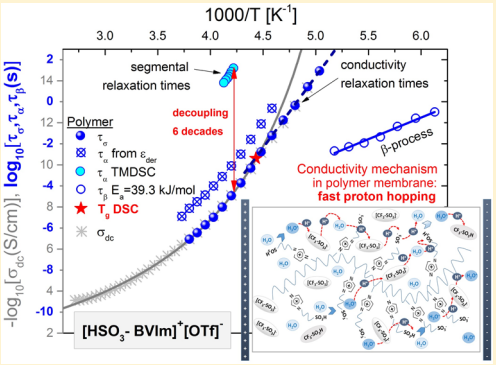

INTRODUCTION

Polymerized ionic liquids (poly-ILs) are a special class of ionic conductors formed by the mobile cations or anions and the repeating counterionic species covalently bonded to the polymer backbone.[1,2] Because of the combination of the unique properties of ionic liquids with macromolecular architecture of polymers, poly-ILs have become attractive candidates for potential applications in energy storage and electrochemical devices.[3−5] The major benefit of using these materials is that one can avoid some disadvantages of liquid electrolytes, such as flammability, which is especially important in the application areas of batteries and fuel cells.[6] Additionally, the polymeric nature of ILs potentially permits production of ion-conductive materials with different size, shape, and geometry, such as thin films.

One of the most attractive research directions in the fields of electrochemistry and material science is the development of polymerized protic ionic liquids (poly-PILs).[7] The long-term thermal stability of these systems together with their high ionic conductivity in anhydrous conditions makes them promising alternative for the water-saturated proton-conducting polymer electrolytes that are characterized by the rapid loss of conductivity at temperatures higher than 100 °C. Additionally, the preparation of poly-PILs is relatively cheap and environment-friendly in contrast to fluorinated ionomer membranes represented by Nafion. Although proton conducting systems possess so many advantages, only a few examples of protic poly-IL-containing materials are reported in the literature.[8−10] Hence, we have recently designed a new polymer membrane based on a protic imidazolium ionic liquid, 1-(4-sulfobutyl)-3-vinylimidazolium trifluoromethanesulfonate [HSO_3−BVIm]-[OTf]. We have found that photopolymerization of [HSO_3−BVIm][OTf] results in a thermally stable solid material (up to 200 °C) that is able to reach current densities of 154 mA/cm^2 and maximum power of 33 mW/cm^2 at 25 °C.[11] However, due to the sulfonate group present in the chemical structure, the examined poly[HSO_3−BVIm][OTf] reveals a high ability to attract and hold water molecules from the surrounding environment. Therefore, it is crucial to identify the effect of water presence on the ion transport properties in the newly synthesized poly-PIL. It is well-known that the acidic groups SO_3H, located in the side chains of polymer electrolyte membranes such as Nafion, exposed to water dissociate into immobile SO_3^- anions and free protons that move through the hydrogen-bonded network of water molecules and thereby are responsible for high conductivity of the system.[12] In this context it is of a considerable interest to examine whether or not a similar mechanism can be considered as the source of high conductivity of poly[HSO_3−BVIm][OTf].

The broadband dielectric spectroscopy (BDS) is a very powerful experimental tool for understanding the molecular-level dynamics in ion-containing liquids and polymers.[13−16] This technique allows the dielectric response to be measured over 12 decades of frequency at different temperatures giving a

Received: February 18, 2014
Revised: April 27, 2014
Published: June 6, 2014

valuable insight into molecular mobility of a polymerized IL, below as well as above its glass transition temperature (T_g).[17] Additionally, our recent results on protic ionic liquids have demonstrated that based on dielectric measurements it is possible to recognize the type of the charge transport mechanism in ionic conductors. Namely, if conductivity of a system is controlled by the fast proton hopping through the H-bond network, according to the so-called Grotthuss mechanism, close to the liquid-glass transition region the examined ionic material exhibits decoupling of ionic conductivity from the structural relaxation.[18] It means that the ionic motions are still very fast when the structural relaxation becomes frozen. This specific separation between the time scale of charge and mass diffusion in the vicinity of T_g is manifested by the characteristic crossover of the temperature dependence of conductivity (σ_{dc}) or conductivity relaxation times (τ_σ) from the Vogel–Fulcher–Tammann-like ($T > T_g$) to Arrhenius behavior ($T < T_g$).[19] Interestingly, this abrupt change in the $\sigma_{dc}(T)$ dependence observed at T_g in the case of low-molecular weight protic ionic liquids has been also recently found for polymerized ILs.[20,23,25] However, it has never been discussed in the context of ion transport mechanism.

In this paper, we present a detailed analysis of the dielectric relaxation behavior of polymerized imidazolium-based protic ionic liquid [HSO_3–BVIm][OTf] over a wide temperature range. The molecular dynamics of the monomer is also examined as a reference. To describe the ion dynamics of studied materials we have chosen the complex electrical modulus $M^*(f)$ and complex conductivity $\sigma^*(f)$ functions. The applied procedure differs to the standard practice where the results of dielectric measurements of poly-IL are analyzed in permittivity representation $\varepsilon^*(f)$, despite the fact that the main relaxation mode, related to segmental dynamics of the polymers chain, is covered by a large contribution of dc-conductivity.[21−26] In our paper, we demonstrate that the employment of the modulus formalism complemented by the results of temperature modulated differential scanning calorimetry not only enables us to characterize the molecular mobility of the studied samples below as well as above their glass transition temperature but also allows the charge transport mechanism responsible for high ionic conductivity of these systems to be described. Finally, we also provide a deep understanding of the effect of water presence on the value of the glass transition temperature, decoupling phenomenon and conductivity mechanism of examined poly[HSO_3–BVIm][OTf].

EXPERIMENTAL SECTION

Materials. 2-Hydroxy-2-methylpropiophenone (Sigma-Aldrich, 97%), 1-vinylimidazole (Sigma-Aldrich, >99%), 1,4-butane sultone (Sigma-Aldrich >99%) and trifluoromethanesulfonic acid (Apollo Scientific, 99%) were commercially available and used without any further pretreatment or prepurification. Acetonitrile (Panreac, >99.7%) was dried with calcium hydride (Merck, synthesis grade) and distilled under argon prior to use.

Synthesis of [HSO_3–BVIm][OTf]. The protic ionic liquid [HSO_3–BVIm][OTf] (Figure 1) was synthesized following a procedure previously described in the literature.[11] A solution of 1-vinylimidazole (157.7 mmol) in dry acetonitrile (50 mL) was introduced into a two-neck 100 mL round flask under an inert atmosphere. The mixture was cooled at 0 °C and 1,4-butane sultone (157.7 mmol) was added dropwise. The mixture was stirred at 85 °C for 5 days to obtain the corresponding zwitterion as a white precipitate that was isolated by filtration, washed with diethyl ether and dried under high vacuum. A stoichiometric amount of trifluoromethanesulfonic acid was added dropwise to a suspension of zwitterion (147.0 mmol) in acetonitrile (50 mL) at 0 °C under an inert atmosphere and the mixture was stirred for 5 h at room temperature. The solvent was removed at low pressure and the obtained ionic liquid was washed with diethyl ether and dried by heating at 50 °C under high vacuum for 12 h.

1-(4-sulfobutyl)-3-vinylimidazolium trifluoromethanesulfonate [HSO_3-BVIm][OTf]

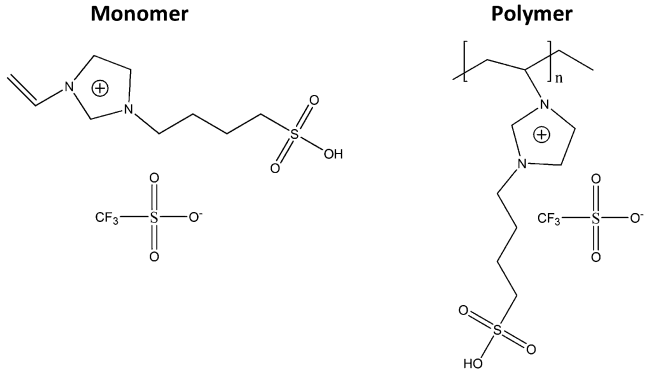

Figure 1. Chemical structures of the examined materials.

Polymerization of [HSO_3–BVIm][OTf]. Ionic liquid monomer [HSO_3–BVIm][OTf] (0.5 g) was mixed with 2 wt % photoinitiator (2-hydroxy-2-methyl propiophenone). The solution was spread over a Petri dish and covered with a quartz plate. This mixture was exposed to 365 nm UV light, with an intensity of 30 mW/cm^2 for 30 min (UV light exposure chamber KAIS). After polymerization, the quartz plate was removed and the film of poly([HSO_3–BVIm][OTf]) was carefully peeled off from the surface using a razor blade. The membrane thickness was measured with a micrometer (Mitutoyo 369–250) which was purchased from Mitutoyo Asia Pacific Pte. Ltd. (Japan) with an accuracy of 0.001 mm (1 μm). For every measurement, at least five points from the different positions of each film were measured and the average value was calculated. The resulting membrane was flexible, transparent and the average thickness was 250–300 μm.

Broadband Dielectric Spectroscopy (BDS). Ambient pressure dielectric measurements of the protic ionic liquid [HSO_3–BVIm][OTf] and its polymer counterpart were performed over a wide frequency range from 10^{-1} to 10^6 Hz using a Novo-Control GMBH Alpha dielectric spectrometer. For the isobaric measurements, the sample was placed between two stainless steel electrodes of the capacitor. The dielectric spectra were collected in a wide temperature range from 153 to 373 K. The temperature was controlled by the Novo-Control Quattro system, with the use of a nitrogen gas cryostat. Temperature stability was better than 0.1 K.

Differential Scanning Calorimetry (DSC). Calorimetric measurements of the studied materials were carried out by a Mettler-Toledo DSC apparatus equipped with a liquid nitrogen cooling accessory and a HSS8 ceramic sensor (a heat flux sensor with 120 thermocouples). Temperature and enthalpy calibrations were performed using indium and zinc standards.

Using a stochastic temperature-modulated differential scanning calorimetry (TMDSC) technique implemented by Mettler-Toledo, TOPEM, the dynamic behavior of the glass–liquid transition of the studied poly-PIL was analyzed in the frequency range from 4 mHz to 40 mHz in a single measurement at a heating rate of 0.5 K/min. In these experiments, the temperature amplitude of the pulses of 0.5 K was selected. The calorimetric segmental relaxation times $\tau_\alpha = 1/2\pi f$ were determined from the temperature dependence of the real part of the complex heat capacity $C_p'(T)$ obtained at different frequencies in the glass transition region. The glass transition temperature T_g was determined for each frequency as the temperature at half the step height of $C_p'(T)$.

Procedure of Water Evaporation from the Polymer Membrane. The poly-PIL sample was prepared in an open aluminum crucible (40

dx.doi.org/10.1021/ma5003479 | Macromolecules 2014, 47, 4056–4065

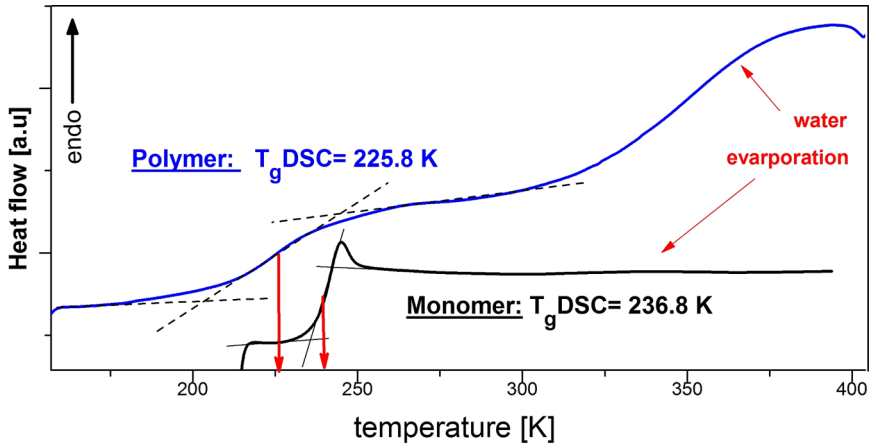

Figure 2. Thermal analysis of imidazolium-based protic ionic liquid [HSO_3−BVIm][OTf] and its macromolecular counterpart. Both DSC thermograms were obtained during heating at a rate of 10 K/min. The values of T_g were determined as the midpoint of the glass transition step in the thermograms.

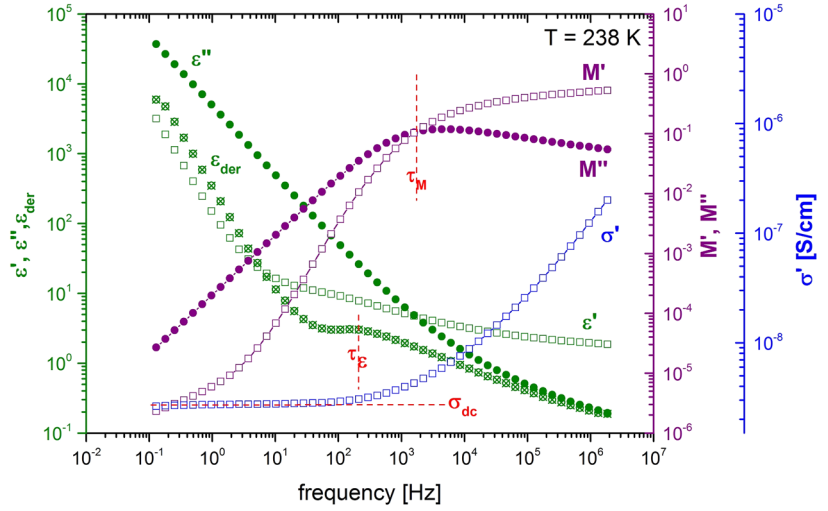

Figure 3. Dielectric relaxation spectrum recorded at 238 K for examined poly-PIL, shown in three equivalent representations: electric modulus, dielectric permittivity, and conductivity. To change the $\varepsilon^*(f)$ formalism into $M^*(f)$ the following formulas were applied: $M'(f) = (\varepsilon'(f))/(\varepsilon'^2(f) + \varepsilon''^2(f))$, $M''(f) = (\varepsilon''(f))/(\varepsilon'^2(f) + \varepsilon''^2(f))$. On the other hand, ε_{der} was calculated using the following equation: $\varepsilon_{der} = -\pi/2\ \partial\varepsilon'(f)/\partial[\ln f]$.

μL) outside the DSC apparatus. First, the polymer membrane with a weight of 13.46 mg was annealed in a vacuum oven for 72 h at 393 K. During this process the sample lost 1.26 mg (9.18 wt %) of water in comparison with the initial sample weight. The aluminum crucible containing such a prepared poly-PIL sample was sealed with the lid having five punctures in order to enable water to volatilize during the sample heating. Next, several calorimetric measurements in the temperature range of 223−523 K at the heating rate of 10 K/min under dry nitrogen purge (60 mL/min) were performed. Each measurement was finished with a 5 min long isothermal scan of the sample at a temperature of 523 K to remove water residue. The examined material was weighed before each measurement, and the content of water remaining in the sample was determined. The above procedure was repeated until the polymer mass and T_g value had become stable. It was determined that the initial water content in the polymer membrane was 11.14 wt %.

RESULTS AND DISCUSSION

A. Thermal Properties of Examined Materials. To provide initial characterization of the examined materials we employed calorimetric measurements. The DSC scans obtained during heating of the monomer and polymerized PIL, up to 400 K, are presented in Figure 2. It can be seen in this plot that the DSC curves reveal heat flow jumps, characteristic of the glass transition temperature, at 225.8 and 236.8 K for the polymer and monomer, respectively. Since the examined compounds are quite hygroscopic, in the thermograms one can also observe broad endotherms related to the water evaporation. However, it can be easily discerned that in the case of poly[HSO_3−BVIm][OTf] this effect is much more pronounced, in comparison with that found for the monomer, due to the higher content of water. The water fraction in the examined materials was determined by the weight difference between the initial sample and that obtained after the drying procedure, as described in the Experimental Section. We have found that the polymerized PIL contains 11.14 wt % of water, while its monomer is characterized by the water content equal to 0.63 wt %. This is the reason why the value of T_g of polymer is lower than that determined for monomer sample. Moreover, it should be noted that the low moisture content of the protic ionic liquid, less than one percent, is a result of the sample storage in anhydrous conditions. The same sample kept in high humidity conditions had 3 wt % of water. The reason why the

dx.doi.org/10.1021/ma5003479 | Macromolecules 2014, 47, 4056−4065

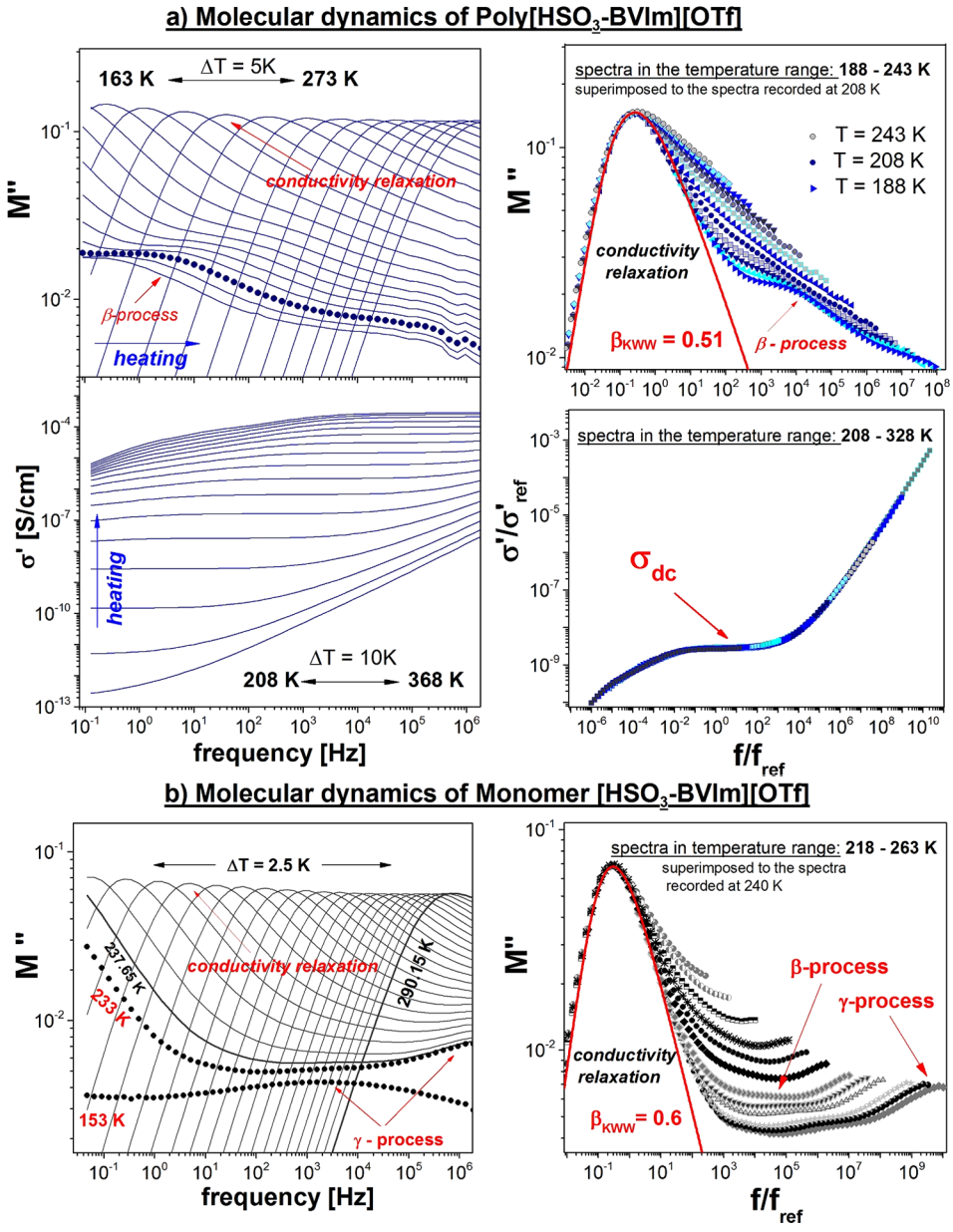

Figure 4. (a) Dielectric relaxation spectra measured above and below the glass transition temperature of poly-PIL presented in modulus and conductivity representations in the form of frequency dependent data as well as the masterplot. (b) M″-dielectric spectra of the monomer sample. The red solid lines are fits of the KWW function to the experimental data.

polymer takes up more water than the monomer is because it has a well-organized structure capable of retaining water inside.

B. Dielectric Relaxation Behavior of Polymerized Protic Ionic Liquid. Generally, dielectric spectra can be presented in three frequency dependent complex quantities: the complex permittivity $\varepsilon^*(f) = \varepsilon'(f) - i\varepsilon''(f)$, the complex conductivity $\sigma^*(f) = \sigma'(f) + i\sigma''(\sigma)$ and the complex electric modulus $M^*(f) = M'(f) + iM''(f)$, which are related to each other according to the following equation:[27]

$$M^*(f) = 1/\varepsilon^*(f) = i2\pi f\varepsilon_0/\sigma^*(f) \quad (1)$$

It should be noted that all these representations emphasize different facets of the same process. Therefore, details which are not readily evident from one approach can be discriminated from the spectra in the other two representations. For most conventional polymers, the dielectric data can be successfully analyzed in the susceptibility formalism. This is because the main relaxation process (related to the segmental dynamics of the polymer chain) that determines the glass transition temperature is visible in the $\varepsilon''(f)$ spectrum in the form of a well-resolved mode.[28−30] On the other hand, in the case of ionic compounds at low frequencies, ionic conductivity gives rise to a sharp increase in the dielectric loss function that completely masks the segmental relaxation within the polymer chain. Consequently, in order to describe the molecular dynamics of ionic polymers the standard practice is to use the derivative formalism, which eliminates the conductivity contribution from the loss spectra.[20−23] This difficulty can be avoided by analyzing the dielectric properties of poly[HSO_3−BVIm][OTf] using the electric modulus $M^*(f)$ and electric conductivity $\sigma^*(f)$ representations which are common approaches to present dielectric data of amorphous conducting materials.[31−35] To better visualize the differences between

dx.doi.org/10.1021/ma5003479 | Macromolecules 2014, 47, 4056−4065

$M^*(f)$, $\sigma^*(f)$, and $\varepsilon^*(f)$ formalisms, a representative BDS spectrum of poly-PIL, measured at 238 K, is shown in all three representations. As demonstrated in Figure 3, the imaginary part of complex modulus takes the form of a well-pronounced peak, so-called a conductivity relaxation peak, in contrast to the $\varepsilon''(f)$ function that suddenly increases with a decreasing frequency. On the other hand, the real part of the complex conductivity is characterized, on the low frequency side, by a plateau (the value of which directly yields the dc conductivity, σ_{dc}) and the power law behavior at higher frequencies. In this context, it noteworthy that the dc-conductivity, usually defined as the product of the number of ions and their mobility, is inversely proportional to the conductivity relaxation times τ_σ (or τ_M) determined from the frequency of M'' peak maximum $\tau_M = 1/(2\pi f_M)$.[27]

Herein, it is worthwhile stressing that physically the electric modulus corresponds to the relaxation of the electric field in the material when the electric displacement remains constant, so that the M^* formalism represents the real dielectric relaxation process. On the other hand, dielectric permittivity ε^* is a magnitude reflecting the relaxation of the electric displacement vector **D**, when the electric field **E** remains constant. Therefore, the susceptibility representation, in contrast to $M^*(f)$, describes the dielectric retardation process.[36] It is also worth noting that the relaxation time τ_M, is in general faster than the retardation time τ_ε, in accordance with the following equation:[37]

$$\tau_M\left(\frac{\varepsilon_s}{\varepsilon_\infty}\right) = \tau_\varepsilon \tag{2}$$

where ε_s and ε_∞ are dielectric constants in the limits of low and high frequency, respectively. Note that eq 2 is valid only for simple Debye-like relaxation. In the case of non-Debye distribution of relaxation times the difference between τ_M and τ_ε becomes even more pronounced. Thus, only for systems with very low dielectric strength and the Debye shape, the difference between the relaxation and retardation time scales becomes negligible. This is the reason why in Figure 3 the M'' maximum is shifted to higher frequencies in comparison with $\varepsilon_{der}(f_{max})$ calculated from the differentiation of the real part of the dielectric permittivity function.

C. Molecular Dynamics of Poly[HSO_3−BVIm][OTf] below and above T_g. Figure 4a depicts dielectric response of poly[HSO_3−BVIm][OTf] measured over seven decades of frequency in a wide temperature range (163−368 K) in both, modulus and conductivity, representations. As one can easily see, in the $M''(f)$ spectra at low temperatures taken from 163 to 203 K there is one clearly visible secondary relaxation (labeled as β-mode), corresponding to some localized motions, that moves toward high frequencies with increasing temperature and it is becoming less pronounced at 208 K. Then, the asymmetric conductivity relaxation peak, originating from the ion motions, becomes the main feature in the spectra. The M'' maximum is observed in the experimental window up to 273 K. This is why above this temperature the dielectric data of poly-PIL are analyzed only in the electric conductivity representation. Interestingly, by superimposing a number of $\sigma'(f)$- conductivity curves, measured at different temperature conditions, on the spectra recorded at 238 K, we obtained the perfect scaling plot with three clearly distinct regions: (1) the frequency independent part of σ' that corresponds to the dc-conductivity, (2) the power law behavior of the real part of the complex conductivity observed at higher frequencies, and (3) the drop of σ' from σ_{dc} value, observed at lower frequencies, due to the electrode polarization process. In contrast to the presented $\sigma'/\sigma'_{ref}(f/f_{ref})$ scaling curve the "masterplot", constructed by using the M''-data taken at different temperatures and shifted horizontally to the approximately one peak position, reveals that the frequency dispersion narrows with decreasing temperature. This is probably due to the lower contribution of β-mode that becomes separated from the high frequency flank of conductivity relaxation. Additionally, one can easily observe that, in contrast to the classical Debye response, the experimentally observed conductivity relaxation peak of poly[HSO_3−BVIm][OTf] is broader and asymmetric. To parametrize the shape of this mode we applied the empirical nonexponential function suggested by Kohlrausch and Williams and Watts given by[38,39]

$$\phi(t) = \exp\left[-\left(\frac{t}{\tau_\sigma}\right)^{\beta_{KWW}}\right] \tag{3}$$

where t is the time, τ_σ is the characteristic conductivity relaxation time and β_{KWW} ($0 < \beta_{KWW} < 1$) denotes the stretching parameter, which is related to the width of the relaxation peak. It is well-known that the broader and more asymmetric the peak is, the lower is the value of β_{KWW} parameter determined from the fitting analysis. The representative fit of the KWW function to the experimental data is shown as a red line in Figure 4a. It should be noted that the value of β_{KWW} equal to 0.51 at 208 K, estimated for the studied herein poly[HSO_3−BVIm][OTf], is close to those obtained for other materials with macromolecular architecture.[27,40] On the other hand, the value of the stretching exponent is lower than that determined for the monomer counterpart of the examined polymer ($\beta_{KWW} = 0.6$), which is also a typical behavior. Interestingly, analysis of the M'' spectra presented in Figure 4b clearly demonstrates that for the monomer, just like in the case of the previously described polymerized PIL, the time−temperature superposition principle is not valid. The examined PIL is a new example confirming the general observation that the conductivity relaxation process for low-molecular weight protic ionic conductors becomes narrow upon cooling.[31,41,42] It is worth to emphasize that the M''-loss spectra recorded for [HSO_3−BVIm][OTf] liquid are characterized by two secondary modes (β and γ), in contrast to one β-process observed for poly-PIL. Moreover, β-relaxation is strongly separated from the conductivity process, thus it cannot be considered as a source of the broadening of the M'' peak observed during the heating of monomer sample. That is why one can suppose that the observed narrowing of the M''-loss peak on cooling may be due to the dynamic fluctuations in the structure (so-called heterogeneous nature of molecular dynamics) of the examined glass-forming liquid.[43]

To provide a detailed description of the molecular dynamics and ionic transport in poly[HSO_3−BVIm][OTf] as well as its low-molecular weight counterpart, in the next step of our analysis, the relaxation times of β-, γ-, and σ-relaxation processes observed in the dielectric loss spectra were calculated from the frequency of M''-peak maximum, f_{max}. As can be easily seen in Figure 5, τ_β and τ_γ exhibit a linear dependence when plotted in a logarithmic scale as a function of $1000/T$. Additionally, the relaxation data points of β-mode, calculated for polymerized PIL and its monomer, fall on the same line. Thus, one can expect that the β-processes, observed in the

dx.doi.org/10.1021/ma5003479 | Macromolecules 2014, 47, 4056−4065

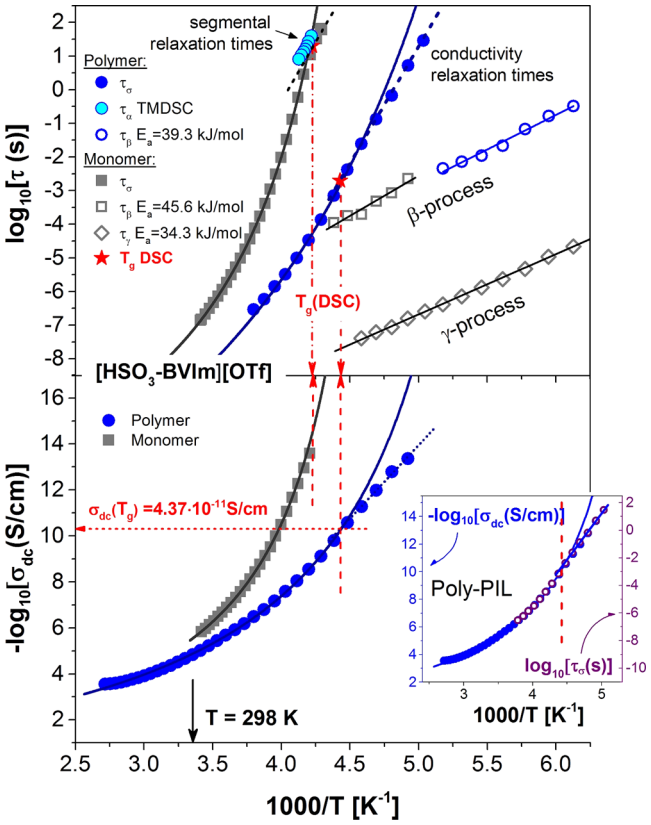

Figure 5. Temperature dependence of τ_σ, τ_β, and τ_γ (upper panel) and dc-conductivity (lower panel) for the polymerized protic ionic liquid and its monomer. The log $\tau_\sigma = f(1000/T)$ dependences are described by the VFT function (above T_g) and Arrhenius law (below T_g). The log τ values for β and γ processes are parametrized by the Arrhenius equation. Red stars denote T_g values determined from standard DSC measurements, while light blue circles indicate the segmental relaxation times τ_α obtained for poly-PIL by the temperature modulated DSC technique. The inset panel presents the log $\sigma_{dc}(1/T)$ and log $\tau_\sigma(1/T)$ data recorded for poly-PIL.

dielectric spectra of both examined samples, are characterized by a similar activation barrier and probably have the same molecular origin. To verify this assumption, in the next step of our analysis from the fit of the Arrhenius equation (eq 4) to the experimental data we determined the activation energy (E_a) of β-modes.

$$\log \tau_\gamma = \log \tau_\infty + \frac{E_a}{RT}\log e \tag{4}$$

E_a of β-modes was found to be equal to 45.6 ± 2.1 kJ/mol and 39.3 ± 0.32 kJ/mol, for PIL and its polymerized counterpart, respectively. It is noteworthy that the both values are in a good agreement with the activation energy barrier estimated for the molecular motions of supercooled water situated in some confined systems ($E_a \approx 44.4 \pm 3.7$ kJ/mol)[44] and various water mixtures, e.g. DPG + H_2O (43 kJ/mol)[45] or a hydrated protic ionic liquid, lidocaine hydrochloride (49.2 kJ/mol).[46] Since the thermal analysis presented in the previous part of this paper clearly indicates that the tested samples are characterized by a quite high water content, one can conclude that the β-relaxation reflects mainly the water dynamics in the examined [HSO_3−BVIm][OTf]-based materials. On the other hand, the lower activation energy barrier of γ-process, determined as 34.3 ± 0.34 kJ/mol, implies that some intramolecular motions are responsible for occurrence of this mode in the modulus loss spectra of the monomer sample. Additionally, the lack of γ-relaxation in the glassy state of poly-PIL indicates that this mode probably comes from the mobility of imidazolium cations that in the polymeric material is highly limited.

To further advance our understanding of the charge transport mechanism in poly-PIL, in the next part of this paper we will explore the temperature dependences of conductivity relaxation times τ_σ and dc-conductivity σ_{dc}. The experimentally determined variations in log τ_σ with temperature are depicted in Figure 5a as open circles and squares, for polymer and PIL respectively. It should be noted that the standard practice is to parametrize the log $\tau_\sigma(T)$ dependence by means of the Vogel−Fulcher−Tammann equation:[47−49]

$$\log \tau_\sigma = \log \tau_0 + \frac{DT_0}{T - T_0}\log e \tag{5}$$

where log τ_0, D, and T_0 are constants. The same procedure was also applied to the studied materials, however, already at the first sight, it is obvious that in these cases the VFT equation does not describe the experimental data satisfactorily over the entire measured temperature range. As depicted in Figure 5a the temperature dependence of conductivity relaxation times, τ_σ, determined for both PIL and its polymer form, changes from VFT-like to Arrhenius behavior. According to the latest reports on protic ionic conductors, the observed crossover is a manifestation of the glass transition behavior of examined ionic glass-formers.[18,19,50,51,33,52] In this context, it should be stressed that the T_g is usually defined as the temperature at which the structural relaxation time, or segmental relaxation time in the case of polymers, τ_α, is equal to 10^3 s.[53] However, the kink of $\tau_\sigma(T)$ curve for polymerized PIL occurs at much shorter conductivity relaxation times, in the order of $\tau_\sigma \sim 0.005$ s. Also, for the monomer the value of τ_σ at T_g is also lower than that traditionally reported. And what is more important, in both these cases the crossover temperatures are in a very good agreement with T_g values determined from standard DSC measurements (see the red stars in Figure 5a). This suggests that, in the case of examined polymerized PIL, there is a significant separation, so-called decoupling, between the time scale of conductivity and segmental relaxation in the vicinity of the glass transition temperature. To explore the relation of ionic transport to segmental dynamics in poly[HSO_3−BVIm][OTf] more quantitatively, we employed temperature-modulated differential scanning calorimetry (TMDSC). This technique, never used before to investigate the dynamics of ionic polymers, enabled us to directly determine the segmental relaxation times τ_α of the examined poly-PIL. As it can be easily seen in Figure 5a, the conductivity relaxation time, describing the ions migration through the polymer matrix, is indeed orders of magnitude faster than its segmental relaxation time. It means that the ions (in this case H^+) might still diffuse when the segmental dynamics is very slow or even completely frozen at T_g. Thus, by combining the dielectric data with the results of TMDSC experiments we explicitly confirmed that in the examined poly-PIL there is a decoupling of proton translation and segmental relaxation process. In this context it should be noted that our findings are in contrast with the standard practice when the crossover between the Arrhenius and VFT behavior of dielectric data is discussed in terms of the ion-pair motions as previously presented in refs 23, 25.

dx.doi.org/10.1021/ma5003479 | Macromolecules 2014, 47, 4056−4065

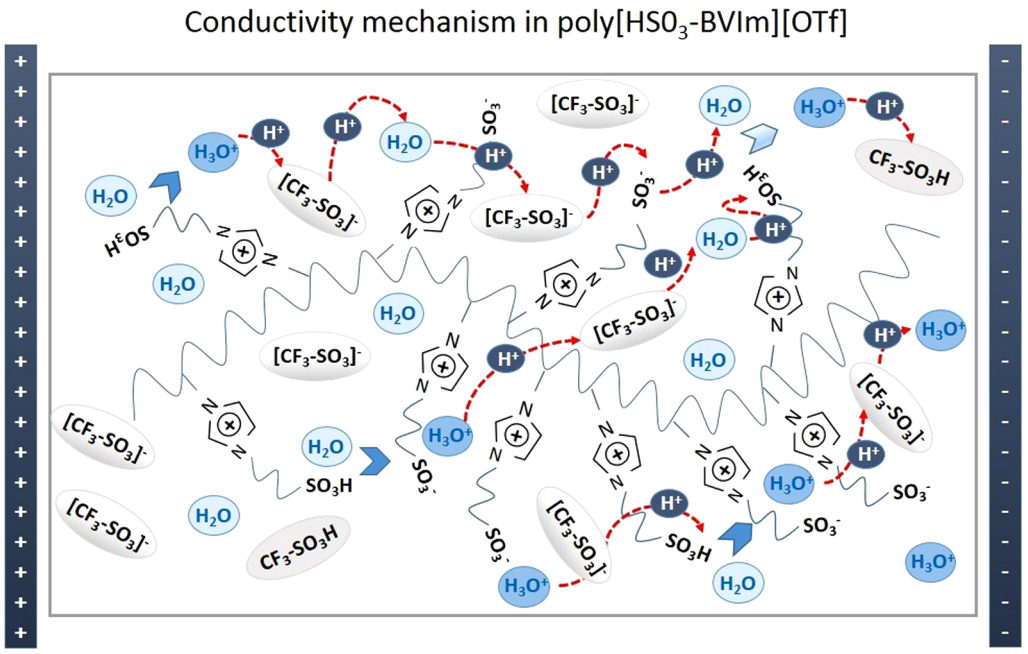

Figure 6. Schematic of the conductivity mechanism in poly-PIL. The sample is placed between the two plates of capacitor. The red arrows indicate the possible pathways of proton hopping in the electric field.

Interestingly, the decoupling between the segmental and conductivity relaxation times is also reflected in the dc-conductivity behavior. As illustrated in the inset to Figure 5b, it does not matter which representation we choose because the temperature dependences of σ_{dc} and τ_σ are practically the same. On the other hand, according to the convention, the ionic conductivity in a system where the ion diffusion is tightly coupled to the structural relaxation is in the order of $\sim 10^{-15}$ S/cm at T_g.[54] However, the $\sigma_{dc}(T_g)$ estimated for the examined herein polymerized protic ionic liquid is several orders of magnitude higher than this value (4.37×10^{-11} S/cm). Moreover, it also exceeds the value of dc-conductivity determined for the monomer in the whole explored temperature range. This observation is in contrast with the general rule which says that the polymerization of ionic liquids results in lower ionic conductivity than that found for the monomer due to both, considerable elevation of glass transition temperature and reduced number of mobile ions after covalent bonding of cations.[55] Consequently, one can expect that different mechanisms are responsible for the conducting properties of the PIL and its polymerized counterpart.

In this context it is notable that generally one can distinguish two types of charge transport mechanisms in protic ionic conductors: vehicle and Grotthuss-type. In the vehicle mechanism the charge transfer is connected with the molecular diffusion. Consequently, the conductivity is controlled by the viscosity of a system. On the other hand, in the Grotthuss mechanism, the charge transport is realized through the proton hopping via the hydrogen bonding network in addition to the translational diffusion of ions.[56,57] Intuitively, the proton migration in the H-bonded systems is much faster than the typical ionic diffusion. Therefore, the Grotthuss mechanism can be considered as a source of both the excess conductivity of polymerized PIL as well as the decoupling phenomenon between τ_α and τ_σ observed in the case of protic ionic conductors examined in this paper. Additionally, one can imply that the greater is the decoupling between the ionic transport and structural/segmental relaxation, the higher is the contribution of fast proton hopping to the conductivity mechanism. As a consequence, one can assume that in the case of the studied imidazolium-based ionic liquid the conductivity is controlled mainly by diffusion of cations and anions in contrast to the polymer where the proton hopping is much more relevant.

To provide a deeper understanding of the charge transport mechanism in polymerized [HSO_3–BVIm][OTf], its chemical structure was closely inspected (Figure 1). The macromolecular architecture of this system is formed by imidazolium cations, terminated by HSO_3 groups and clipped to the alkyl polymer chain from the other side, and trifluoromethanesulfonate anions ($CF_3SO_3^-$). Because of the sulfonate groups present in the chemical structure of both counterions, the examined material is essentially a strong polymer acid. Thus, when exposed to water, it dissociates into immobile ionomers SO_3^- residing on the side chains of the polymer and free mobile protons. As it was proved above by DSC, the synthesized poly[HSO_3–BVIm][OTf] is a highly water-saturated macromolecular system that contains 11.14 wt % of water. Therefore, in the polymer matrix there are plenty of mobile protons that can easily jump through the dense H-bonded network formed by ions and water molecules. Consequently, the polymer membrane is in fact a mixture of imidazolium-based zwitterions linked to the alkyl chain, $CF_3SO_3^-$ and H_3O^+ ions as well as neutral molecules of trifluoromethanesulfonic acid (TFSA) and water. To visualize the possible pathways of proton migration in poly-PIL matrix, the structure of studied material is schematically illustrated in Figure 6. In the light of the presented results, it is obvious that the high conductivity of the examined polymerized protic ionic liquid is mainly due to the mobile protons that are released during dissociation of HSO_3 groups. Consequently, the σ_{dc} value is expected to decrease when the amount of water is limited. However, the question about the glass transition temperature, decoupling phenomenon and conductivity mechanism in anhydrous poly-PIL remains

dx.doi.org/10.1021/ma5003479 | Macromolecules 2014, 47, 4056–4065

still unanswered. To shed more light on this issue in the next part of this paper we will focus on the molecular dynamics studies of poly-PIL that contains a reduced content of water.

D. Effect of Water on the Molecular Mobility of Polymerized PIL. It has been frequently reported that even a small amount of water absorbed by low molecular weight ionic conductors may have a great impact on their molecular dynamics and ion transport.[50,51] Numerous studies have shown that water, in general, strongly reduces the glass transition temperature of an ionic system and increases the conductivity of solution.[58,59] However, the discussion about an influence of water on the decoupling between charge and mass diffusion is highly limited. The only information about this phenomenon comes from our recent paper on PIL lidocaine hydrochloride monohydrate where we have found that at ambient pressure conditions the decoupling observed for the hydrated sample and its anhydrous analogue is practically the same.[46] In this context, it is of great interest to investigate, for the first time, the influence of water on the relation between conductivity relaxation times and segmental dynamics of polymerized protic ionic liquid.

To realize this task it is crucial to remove water from the examined poly-PIL sample. However, it was determined that it is quite difficult to prepare a completely anhydrous material. We found that even after 72 h annealing at 393 K in a vacuum oven the examined poly-PIL still contained 1.96 wt % of water. To obtain a completely dry poly[HSO_3−BVIm][OTf] sample, heating at much higher temperatures, in the order of 523 K, for approximately half hour was required. However, it should be noted that the applied procedure resulted in a change of the sample color from beige to brown. Additionally, the thermogravimetric analysis of examined poly-PIL has revealed a slight mass loss around 473 K. Since these facts can be associated with the partial decomposition of poly-PIL, for further studies we used the polymer membrane that contained 1.96 wt % of water. The DSC thermogram obtained during the heating of such prepared material is depicted in the inset panel of Figure 7. As it can be easily seen, the characteristic signature of the glass transition is observed in the temperature dependence of the heat flow at 305 K. Interestingly, this value is 13 K lower than that determined for the anhydrous polymer membrane and 80 K higher in comparison with the previously examined hydrated sample. Markedly, this is the first report when such a dramatic decrease in T_g, due to the water presence, was obtained for a polymerized protic ionic conductor.

Now we will focus on the molecular dynamics studies of poly[HSO_3−BVIm][OTf] sample with the reduced content of water (1.96 wt %). The dielectric spectra recorded in a wide temperature range (both above and below T_g) for the dried polymer are presented in the form of mastercurve in the inset panel of Figure 8. As illustrated in this plot, the loss component of the complex electric modulus, deep in the glassy state is characterized by two well-resolved secondary processes, β and γ. However, with increasing temperature these two modes are getting hardly visible, which makes the further analysis of log $\tau_{\beta\gamma}$ = $f(1/T)$ impossible. On the other hand, from comparison of the modulus loss spectra collected above T_g, it is clearly seen that the σ-process slightly broadens with the increase of temperature, just like it was observed for the hydrated polymer membrane. In order to analyze the data more quantitatively we compared two dielectric curves, collected for dried and hydrated polymer samples, in the one plot. The spectra were

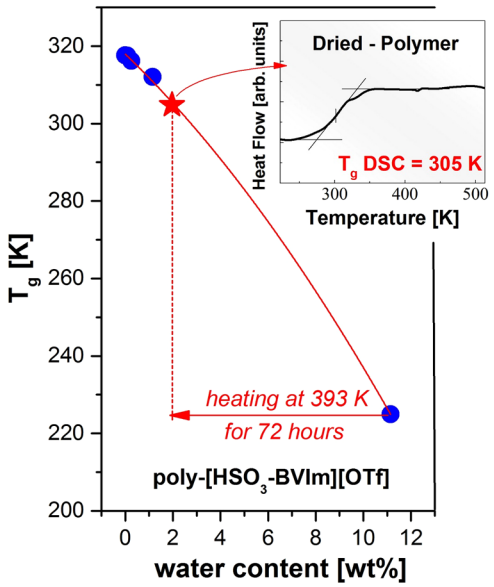

Figure 7. Glass transition temperature as a function of water content determined for polymerized PIL. In the inset panel, depicts the temperature dependence on the heat flow for the material with 1.96 wt % of water.

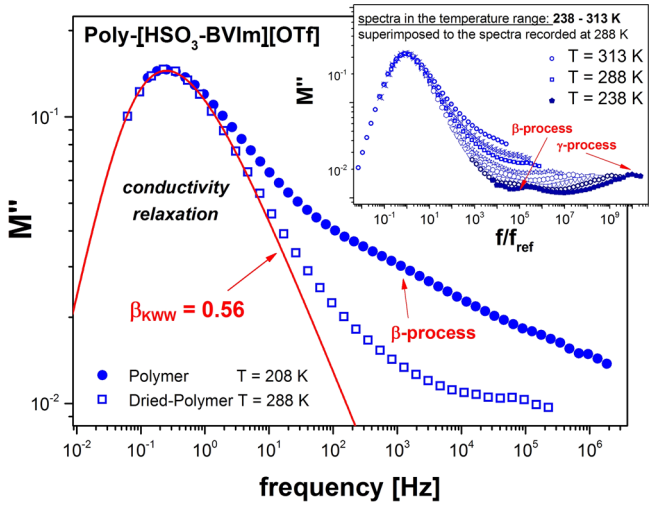

Figure 8. Comparison of dielectric spectra with the same σ-relaxation times obtained at different temperatures for the hydrated polymer (solid circles) and dried membrane (open squares). The inset panel presents superimposed dielectric spectra of the dried polymer taken at different temperatures above and below T_g.

chosen so that the frequencies of the σ-relaxation peak maximum were the same. From the inspection of $M''(f)$ data presented in Figure 8 it becomes obvious that the high frequency side of the σ-mode becomes narrower with the decrease of water fraction (the stretching exponent in KWW function increases from 0.51 to 0.56). Moreover, it can be easily seen that the intensity of the β-peak has markedly decreased when the amount of water was reduced. These results confirm our previous statements that (i) β-relaxation indeed reflects the dynamics of water molecules in polymer matrix and (ii) the broadening of M''-spectra for the hydrated membrane is mainly due to the high contribution of the β-relaxation peak.

To explore the effect of water presence on the ion transport properties of the dried poly[HSO_3−BVIm][OTf] sample in the

dx.doi.org/10.1021/ma5003479 | Macromolecules 2014, 47, 4056−4065

next step of our analysis we determined the temperature dependences of dc-conductivity and conductivity relaxation times. Similar to the highly hydrated material, the values of σ_{dc} were evaluated directly from the region where the real part of complex conductivity is constant, while τ_σ was estimated from the frequency of modulus peak maximum. As it can be easily seen in Figure 9b, evaporation of water from the polymer

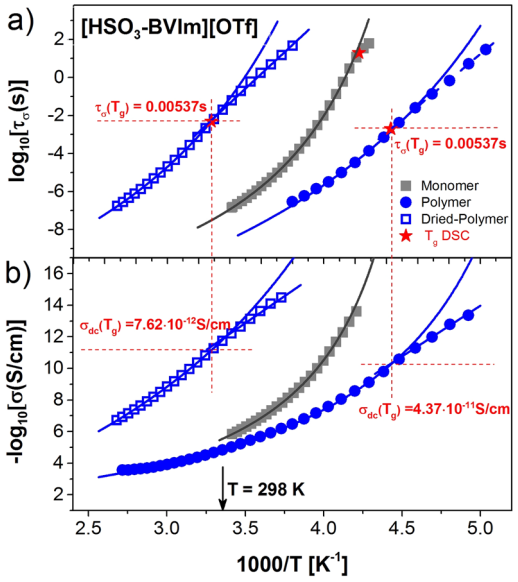

Figure 9. Temperature dependence of τ_σ, (upper panel) and dc-conductivity (lower panel) for the hydrated polymerized protic ionic liquids (solid circles), dried polymer membrane (open squares) and monomer (solid squares). Red stars denote T_g values determined from DSC measurements.

matrix results in a dramatic decrease of σ_{dc}. At room temperature it drops by several orders of magnitude, from 1.25×10^{-5} to 1.76×10^{-12} S/cm. Additionally, in the whole examined temperature range, it is lower than the conductivity of nonpolymerized PIL, which is now in agreement with the Ohno theory.[55] However, close to the glass transition region, where the viscosity of both polymer samples is approximately equal to 10^{12} Pa·s, the values of σ_{dc} are also the same. Interestingly, the kink of $\tau_\sigma(T)$ dependence from VFT-like to Arrhenius behavior, determined for dried poly-PIL, occurs at practically the same conductivity relaxation times as for the hydrated sample ($\tau_\sigma \sim 0.005$ s) (see Figure 9a). It means that the charge transport in the annealed poly[HSO_3–BVIm][OTf], is still faster than the segmental dynamics and consequently, the conducting properties of the examined dried-polymer are still governed by the fast proton hopping through the H-bond network. However, one should note that in this case the number of charge carriers (protons) in the polymer membrane is significantly reduced due to the limited content of water. Herein, one should note that due to the delocalization of proton in the imidazolium cation, even in the absence of water, the conducting properties of the examined poly[HSO_3–BVIm][OTf] membrane can be controlled by the Grotthuss mechanism. That is why it can be assumed that in the case of a completely anhydrous poly-PIL sample, the $\sigma_{dc}(T_g)$ value remains the same. Consequently, using protic ionic liquids as a polyelectrolyte one can avoid the serious problem of water management observed for commercial membranes for low temperature fuel cell applications.

CONCLUSIONS

In this paper, we have outlined a completely new approach to the dielectric relaxation studies of polymerized ionic conductors in general. On the basis of the BDS experimental data combined with the results of differential scanning calorimetry (DSC) measurements, collected for [HSO_3–BVIm][OTf] polymer membrane and its monomer, one can draw the following conclusions:

1. The complex electrical modulus $M^*(f)$ function is an appropriate formalism to analyze the dielectric spectra of both polymerized ionic liquid and its low-molecular weight counterpart. Using this representation we were able to describe the molecular mobility of the examined materials in the glassy state as well as to provide a thorough understanding of the charge transport mechanism responsible for high ionic conductivity of these systems. This information would be lost if the data were presented only in terms of $\sigma^*(f)$ or $\varepsilon^*(f)$ representations.
2. The large decoupling between the conductivity relaxation times τ_σ and segmental dynamics (τ_α) observed for [HSO_3–BVIm][OTf] polymer membrane in the vicinity of T_g is an evidence that the conductivity of the studied poly-PIL is controlled by the fast proton hopping via the H-bond network, according to the so-called Grotthuss mechanism, in contrast to the monomer where the diffusion of cations and anions is relevant.
3. From the molecular dynamics studies of two poly-PIL–water mixtures, we found that even a small amount of water absorbed by an ionic conductor results in the β-secondary relaxation visible in the M'' loss spectra recorded below T_g. The characteristic feature of this mode is its activation energy (E_a) approximately equal to 40 ± 10 kJ/mol (39.3 and 45.6 kJ/mol for the examined PIL and its polymerized counterpart, respectively) and amplitude dependent on the water content.
4. The log $\tau_\sigma(T)$ dependence, determined for poly[HSO_3–BVIm][OTf] membrane, strongly depends on the water content. This effect is clearly visible in the value of T_g, which decreases almost 80 K with an increase the water fraction from 1.96 to 11.14 wt %. Interestingly, despite the dramatic drop in the water content the kink of $\tau_\sigma(T)$ dependence from VFT-like to Arrhenius behavior occurs at practically the same conductivity relaxation times. Furthermore, the value of $\sigma_{dc}(T_g)$ also remains unchanged. These facts suggest that regardless of the amount of water present in the sample the charge transport mechanism of the examined herein polymer membrane is permanently governed by fast proton hopping.

AUTHOR INFORMATION

Corresponding Author

*(Z.W.) E-mail: zaneta.wojnarowska@us.edu.pl.

Notes

The authors declare no competing financial interest.

ACKNOWLEDGMENTS

Z.W. and M.P. are deeply grateful for the financial support by the National Science Centre within the framework of the Maestro2 project (Grant No. DEC-2012/04/A/ST3/00337). Z.W. acknowledges financial assistance from FNP START.

M.D., A.O., and I.O. would like to acknowledge the Ministry of Education for financial support under Project CTQ2012-31639 (MINECO, Spain-FEDER 2007-2013). M.D. also thanks the FPU for a fellowship (FPU2012-3721). The authors thank Dr. L. Tajber for critical reading of the manuscript.

REFERENCES

(1) Ohno, H. *Bull. Chem. Soc. Jpn.* **2006**, *79*, 1665.
(2) Mecerreyes, D. *Prog. Polym. Sci.* **2011**, *36*, 1629.
(3) Kim, T. Y.; Lee, H. W.; Stoller, M.; Dreyer, D. R.; Bielawski, C. W.; Ruoff, R. S.; Suh, K. S. *ACS Nano* **2011**, *5*, 436.
(4) Weber, R. L.; Ye, Y.; Schmitt, A. L.; Banik, S. M.; Elabd, Y. A.; Mahanthappa, M. K. *Macromolecules* **2011**, *44*, 5727−35.
(5) Marcilla, R.; Mecerreyes, D.; Winroth, G.; Brovelli, S.; Yebra, M. M. R.; Cacialli, F. *Appl. Phys. Lett.* **2010**, *96*, 043308.
(6) Xu, K. *Chem. Rev.* **2004**, *104*, 4303.
(7) Schneider, Y.; Modestino, M. A.; McCulloch, B. L.; Hoarfrost, M. L.; Hess, R. W.; Segalman, R. A. *Macromolecules* **2013**, *46* (4), 1543−1548.
(8) Feng, Yan; Shaomei, Yu; Xingwang, Zhang; Lihua, Qiu; Fuqiang, Chu; Jingbi, You; Jianmei, Lu *Chem. Mater.* **2009**, *21* (8), 1480−1484.
(9) Yuan, J.; Antonietti, M. *Polymer* **2011**, *52*, 1469e1482.
(10) Moreno, M.; Aboudzadeh, A. M.; Barandiaran, M. J.; Mecerreyes, D. *J. Polym. Sci., Part A: Polym. Chem.* **2012**, *50*, 1049−1053.
(11) Díaz, M.; Ortiz, A.; Vilas, M.; Tojo, E.; Ortiz, I. *Int. J. Hydrogen Energy* **2014**, *39* (8), 3970−3977.
(12) Eikerling, M.; Kornyshev, A. A.; Kuznetsov, A. M.; Ulstrup, J.; Walbran, S. *J. Phys. Chem. B* **2001**, *105*, 3646−3662.
(13) Yu, Y.; Beichel, W.; Dlubek, G.; Krause-Rehberg, R.; Paluch, M.; Pionteck, J.; Pfefferkorn, D.; Bulut, S.; Friedrich, C.; Pogodina, N.; Krossing, I. *Phys. Chem. Chem. Phys.* **2012**, *14*, 6856.
(14) Wojnarowska, Z.; Paluch, M.; Grzybowski, A.; Adrjanowicz, K.; Grzybowska, K.; Kaminski, K.; Wlodarczyk, P.; Pionteck, J. *J. Chem. Phys.* **2009**, *131*, 104505.
(15) Jarosz, G.; Mierzwa, M.; Zioło, J.; Paluch, M.; Shirota, H.; Ngai, K. L. *J. Phys. Chem. B* **2011**, *115* (44), 12709−12716.
(16) Rivera-Calzada, A.; Kaminski, K.; Leon, C.; Paluch, M. *J. Phys.: Cond. Matter* **2008**, *20*, 244107.
(17) Runt, J., Fitzgerald, J. J., Eds. *Dielectric Spectroscopy of Polymeric Materials: Fundamentals and Applications*; American Chemical Society: Washington, DC, 1997.
(18) Wojnarowska, Z.; Wang, Y.; Pionteck, J.; Grzybowska, K.; Sokolov, A. P.; Paluch, M. *Phys. Rev. Lett.* **2013**, *111*, 225703.
(19) Wojnarowska, Z.; Roland, C. M.; Swiety-Pospiech, A.; Grzybowska, K.; Paluch, M. *Phys. Rev. Lett.* **2012**, *108*, 015701.
(20) Choi, U. H.; Ye, Y.; de la Cruz, D. S.; Liu, W.; Winey, K. I.; Elabd, Y. A.; Runt, J.; Colby, R. H. *Macromolecules* **2014**, *47* (2), 777−790.
(21) Nakamura, K.; Saiwaki, T.; Fukao, K. *Macromolecules* **2010**, *43*, 6092−6098.
(22) Nakamura, K.; Saiwaki, T.; Fukao, K.; Inoue, T. *Macromolecules* **2011**, *44*, 7719−7726.
(23) Nakamura, K.; Fukao, K.; Inoue, T. *Macromolecules* **2012**, *45*, 3850−3858.
(24) Smith, T. W.; Zhao, M.; Yang, F.; Smith, D.; Cebe, P. *Macromolecules* **2013**, *46* (3), 1133−1143.
(25) Nakamura, K.; Fukao, K. *Polymer* **2013**, *54*, 3306e3313.
(26) Choi, U. H.; Mittal, A.; Price, T. L.; Gibson, H. W.; Runt, J.; Colby, R. H. *Macromolecules* **2013**, *46*, 1175−1186.
(27) Kremer, F., Schoenhals, A. *Broadband Dielectric Spectroscopy*; Springer: Berlin, 2003.
(28) Viciosa, M. T.; Dionísio, M.; Gómez Ribelles, J. L. *Polymer* **2011**, *52* (9), 1944−1953.
(29) Grzybowska, K.; Wojnarowska, Z.; Grzybowski, A.; Paluch, M.; Giussi, J. M.; Cortizo, M. S.; Blaszczyk-Lezak, I.; Mijangos, C. *Polymer* **2014**, *55* (4), 1040−1047.
(30) Paluch, M.; Pawlus, S.; Roland, C. M. *Macromolecules* **2002**, *35* (19), 7338−7342.
(31) Wojnarowska, Z.; Swiety-Pospiech, A.; Grzybowska, K.; Hawelek, L.; Paluch, M.; Ngai, K. *J. Chem. Phys.* **2012**, *28* (13616), 164507.
(32) Paluch, M.; Haracz, S.; Grzybowski, A.; Mierzwa, M.; Pionteck, J.; Riveera-Calzada, A.; Leon, C. *J. Phys. Chem. Lett.* **2010**, *1*, 987−992.
(33) Wang, Y.; Lane, N. A.; Sun, C.; Fan, F.; Zawodzinski, T. A.; Sokolov, A. P. *J. Phys. Chem. B* **2013**, *117* (26), 8003−8009.
(34) Sangoro, J. R.; Kremer, F. *Acc. Chem. Res.* **2012**, *45*, 525.
(35) Roling, B. *J. Non-Cryst. Solids* **1999**, *244*, 34−43.
(36) Hodge, I. M.; Ngai, K. L.; Moynihan, C. T. *J. Non-Cryst. Solids* **2005**, *351*, 104.
(37) Ngai,K. L. *Relaxation and Diffusion in Complex Systems*; Springer: Berlin, 2011
(38) Kohlrausch, R. *Ann. Phys. (Leipzig)* **1847**, *72*, 393.
(39) Williams, G.; Watts, D. C. *Trans. Faraday Soc.* **1970**, *66*, 80−85.
(40) Van Krevelen, D. W.; *Properties of Polymers*; Elsevier: Amsterdam, 1997.
(41) Wojnarowska, Z.; Roland, C. M.; Kolodziejczyk, K.; Swiety-Pospiech, A.; Grzybowska, K.; Paluch, M. *J. Phys. Chem. Lett.* **2012**, *3*, 1238.
(42) Wojnarowska, Z.; Kołodziejczyk, K.; Paluch, K. J.; Tajber, L.; Grzybowska, K.; Ngai, K. L.; Paluch, M. *Phys. Chem. Chem. Phys.* **2013**, *21* (15(23)), 9205−9211.
(43) Paluch, M.; Wojnarowska, Z.; Hensel-Bielowka, S. *Phys. Rev. Lett.* **2013**, *110*, 015702.
(44) Cerveny, S.; Schwartz, G. A.; Alegría, A.; Bergman, R.; Swenson. *J. Chem. Phys.* **2006**, *124*, 194501.
(45) Grzybowska, K.; Grzybowski, A.; Zioło, J.; Paluch, M.; Capaccioli, S. *J. Chem. Phys.* **2006**, *125*, 044904.
(46) Wojnarowska, Z.; Grzybowska, K.; Hawelek, L.; Swiety-Pospiech, A.; Masiewicz, E.; Paluch, M.; Sawicki, W.; Chmielewska, A.; Bujak, P. *Mol. Pharmacol.* **2012**, *9*, 1250−1261.
(47) Vogel, H. *Phys. Z.* **1921**, *22*, 645.
(48) Fulcher, G. S. *J. Am. Ceram. Soc.* **1925**, *8*, 339.
(49) Tammann, G.; Hesse, W. *Anorg. Allg. Chem.* **1926**, *156*, 245.
(50) Swiety-Pospiech, A.; Wojnarowska, Z.; Hensel-Bielowka, S.; Pionteck, J.; Paluch, M. *J. Chem. Phys.* **2013**, *138*, 204502.
(51) Swiety-Pospiech, A.; Wojnarowska, Z.; Pionteck, J.; Pawlus, S.; Grzybowski, A.; Hensel-Bielowka, S.; Grzybowska, K.; Szulc, A.; Paluch, M. *J. Chem. Phys.* **2012**, *136*, 224501.
(52) Wojnarowska, Z.; Wang, Y.; Paluch, K. J.; Sokolov, A. P.; Paluch, M. *Phys. Chem. Chem. Phys.* **2014**, *16*, 9123.
(53) Floudas, G.; Paluch, M.; Grzybowski, A.; Ngai, K. L. In *Molecular Dynamics of Glass-Forming Systems: Effects of Pressure*; Kremer, F., Ed.; Advances in Dielectrics; Springer-Verlag: Berlin, 2011.
(54) Mizuno, F.; Belieres, J. P.; Kuwata, N.; Pradel, A.; Ribes, M.; Angell, C. A. *J. Non-Cryst. Solids* **2006**, *352*, 5147−5155.
(55) Ohno, H.; Ito, K. *Chem. Lett.* **1998**, *27*, 751.
(56) Kreuer, K. D. *Chem. Mater.* **1996**, *8*, 610.
(57) Angell, C. A. *Solid State Ionics* **1986**, *18−19*, 72−88.
(58) Anouti, M.; Jacquemin, J.; Porion, P. *J. Phys. Chem. B* **2012**, *116*, 4228−4238.
(59) Dobrynin, A. V.; Rubinstein, M. *Prog. Polym. Sci.* **2005**, *30*, 1049.